Transport in Porous Media (2007) 67:1–15
DOI 10.1007/s11242-006-0009-9

Determination of Capillary Pressure Function from Resistivity Data

KEWEN LI[1,⋆] and WADE WILLIAMS[2]
[1]*Stanford University, Yangtze University, Jingzhou, China*
[2]*Core Lab, Inc, USA*

(Received: 15 July 2005; accepted in final form: 24 January 2006)

Abstract. A model has been derived theoretically to correlate capillary pressure and resistivity index based on the fractal scaling theory. The model is simple and predicts a power law relationship between capillary pressure and resistivity index ($P_c = p_e \cdot I^{\beta}$) in a specific range of low water saturation. To verify the model, gas-water capillary pressure and resistivity were measured simultaneously at a room temperature in 14 core samples from two formations in an oil reservoir. The permeability of the core samples ranged from 0.028 to over 3000 md. The porosity ranged from less than 8% to over 30%. Capillary pressure curves were measured using a semi-permeable porous-plate technique. The model was tested against the experimental data obtained in this study. The results demonstrated that the model could match the experimental data in a specific range of low water saturation. The experimental results also support the fractal scaling theory in a low water saturation range. The new model developed in this study may be deployed to determine capillary pressure from resistivity data both in laboratories and reservoirs, especially in the case in which permeability is low or it is difficult to measure capillary pressure.

Key words: capillary pressure, resistivity, well logging, mathematical model, fractal scaling.

Nomenclature

a	constant
b	constant
D_f	fractal dimension of the rock surface
F	formation factor
I	resistivity index
k	permeability
ρ_g	density of rock
m	cementation exponent
n	saturation exponent
P_c	capillary pressure
P_{cD}	dimensionless capillary pressure

⋆Author for correspondence: e-mail: kewenli@stanford.edu

p_e entry capillary pressure
R_0 resistivity of rock at a water saturation of 100%
R_t resistivity of rock at a specific water saturation of S_w
R_w resistivity of water
S_w wetting phase saturation
S_{wc} critical water saturation
S_{wr} residual water saturation
ϕ porosity
β exponent in the relation between disjoining pressures and film thickness

1. Introduction

Both capillary pressure and resistivity index are important parameters in reservoir engineering. It is easier to measure resistivity than capillary pressure in a laboratory, especially for core samples with low permeabilities. One can run resistivity well logging in a well, even in real time, but cannot do this for capillary pressure. It would be useful if a relationship between capillary pressure and resistivity can be found. Resistivity, capillary pressure, and relative permeability have similar features. For example, all are a function of fluid saturation in a porous medium and are influenced by pore structure and heterogeneity. Li (2005) derived a model to infer relative permeability from resistivity index. We speculated that capillary pressure may also be derived from resistivity index.

Szabo (1974) proposed a linear model to correlate capillary pressure with resistivity by assuming the exponent of the relationship between capillary pressure and water saturation is equal to that of the relationship between resistivity and water saturation. This assumption may not be reasonable in many cases. The linear model proposed by Szabo (1974) can be expressed as follows:

$$\frac{R_t}{R_0} = a + bP_c \tag{1}$$

where R_0 is the resistivity of rock at a water saturation of 100%, R_t is the resistivity at a specific water saturation of S_w, P_c is the capillary pressure, a and b are two constants.

The results from Szabo (1974) demonstrated that a single straight line, as predicted by the model (Equation 1), could not be obtained for the relationship between capillary pressure and resistivity index. Longeron *et al.* (1989) measured the resistivity index and capillary pressure under reservoir conditions simultaneously. Longeron *et al.* (1989) didn't attempt to correlate the two parameters.

Literature on the relationship between capillary pressure and resistivity index has been scarce. In this study, a theoretical relationship between capillary pressure and resistivity index was derived according to the fractal

modeling of porous media. In order to verify the relationship experimentally, gas-water capillary pressure and resistivity were measured simultaneously in 14 core samples at a room temperature using a semiporous-plate approach.

2. Theoretical Background

A theoretical relationship between capillary pressure and resistivity index is derived in this section. The basic idea behind this is that both capillary pressure and resistivity index are a function of the wetting phase saturation and the functions are known from the fractal modeling of a porous medium.

Toledo *et al.* (1994) reported that resistivity obeys the scaling law at low wetting phase saturations:

$$\frac{1}{R_t} \propto (S_w)^{\frac{1}{\beta(3-D_f)}} \tag{2}$$

where β is the exponent in the relation between disjoining pressures and film thickness, S_w is the wetting phase saturation, and D_f is the fractal dimension of the rock surface.

Toledo *et al.* (1994) also reported that capillary pressure follows the scaling law at low wetting phase saturations:

$$S_w \propto (P_c)^{-(3-D_f)} \tag{3}$$

Note that a very limited number of experimental data were presented by Toledo *et al.* (1994) to prove the validity of the model represented in Equation 3. The verification of Equation 3 will be conducted later using the experimental data of capillary pressure measured in this study. The relationship between water saturation and capillary pressure can also be represented using different models such as the Brooks and Corey model (1966) and the Van Genuchten Model (1980). In this study, our focus was on the low water saturation range in which the fractal law applies.

Combining Equations 2 and 3, one can obtain:

$$P_c \propto (R_t)^{\beta} \tag{4}$$

It is known that R_t is equal to R_0 when P_c is equal to the entry capillary pressure (p_e) at a water saturation of 100%, which can be expressed as follows using Equation 4

$$p_e \propto (R_0)^{\beta} \tag{5}$$

Combining Equations 4 and 5

$$P_c = p_e \left(\frac{R_t}{R_0} \right)^{\beta} \tag{6}$$

Using the dimensionless form, Equation 6 can be expressed as follows:

$$P_{cD} = (I)^{\beta} \tag{7}$$

where P_{cD} is the dimensionless capillary pressure (P_c/p_e); I is the resistivity index. One can see from Equation 7 that the relationship between capillary pressure and resistivity index is a power law function. Note that this is only warranted in a specific range of low wetting phase saturations, theoretically.

The resistivity index, as a function of the wetting phase saturation, can be represented using the Archie's equation (1942):

$$I = \frac{R_t}{R_0} = S_w^{-n} \tag{8}$$

here n is the saturation exponent. R_0 depends on the porosity of a porous medium and can be calculated (Archie, 1942):

$$F = \frac{R_0}{R_w} = \phi^{-m} \tag{9}$$

where R_w is the resistivity of water, m the cementation exponent, ϕ the porosity, and F the formation factor.

According to Equation 7, dimensionless capillary pressure can be inferred from the resistivity well logging data once the value of β is known. This may provide a new approach obtaining capillary pressure data for reservoir engineering.

3. Experiments

Experiments were conducted at a room temperature to measure gas-water capillary pressure and resistivity simultaneously. The apparatus, rock and fluid properties are described in this section.

3.1. ROCK AND FLUID PROPERTIES

The properties of the core samples used in this study are listed in Table 1. All the core samples were sandstones and were obtained from one oil reservoir but different formations. Group 1 core samples were from one formation with a high permeability and Group 2 were from another formation with a low permeability. The permeability in Group 1 ranged from 437 to 3680 md; the permeability in Group 2 ranged from 0.028 to 387 md.

Table I. Properties of core sample

Core No.	ϕ(f)	k(md)	ρ_g	F	S_{wr}(f)	m	n	S_{wc}(f)	D_f	β	R^2
Group 1											
1	0.272	941	2.66	10.4	0.112	1.80	1.87	0.276	2.749	2.697	0.99
3	0.281	1192	2.66	8.41	0.116	1.68	1.86	0.156	2.952	9.417	0.99
6	0.191	999	2.65	15.5	0.134	1.65	1.82	0.268	2.814	2.926	0.91
8	0.227	3680	2.65	11.8	0.067	1.67	2.00	0.368	2.657	1.255	0.98
10	0.321	437	2.65	8.00	0.167	1.83	2.11	0.265	2.843	2.854	0.96
16	0.262	1916	2.66	9.27	0.078	1.66	1.97	0.298	2.796	2.000	0.95
Group 2											
152	0.114	1.49	2.63	122.3	0.519	2.21	2.49	0.847	2.599	2.491	0.92
153	0.077	0.028	2.64	380.9	0.796	2.32	2.39	0.999	2.824	5.698	0.98
204	0.179	0.560	2.69	43.9	0.617	2.20	1.82	0.943	2.364	1.572	0.92
299	0.185	4.63	2.66	40.4	0.446	2.19	2.13	0.962	2.478	1.914	0.98
334	0.234	387.	2.65	18.5	0.222	2.00	2.02	0.692	2.287	1.402	0.98
336	0.163	35.3	2.66	40.1	0.388	2.03	2.23	0.703	2.388	1.634	0.95
418	0.211	74.0	2.70	26.0	0.454	2.09	2.26	0.926	2.460	1.850	0.99
479	0.210	28.3	2.68	29.9	0.560	2.18	1.91	0.917	2.701	3.349	0.98

f represents fraction.

The brine used for Group 1 core samples had a salinity of 90,000 ppm with a resistivity of 0.078 Ω-m at 25°C. The brine used for Group 2 core samples had a salinity of 20000 ppm with a resistivity of 0.308 Ω-m at 25°C.

3.2. APPARATUS

The schematic of the apparatus used for the combined measurements of gas-water capillary pressure and resistivity is shown in Figure 1. The outside diameter of each porous plate was painted with silver paint. The resistivity meter was manufactured by Quad Tech and the model was 1730 LCR. The frequency used in this study was 20000 Hz.

3.3. EXPERIMENTAL PROCEDURE

The samples designated for these analyses were cleaned and dried prior to testing. Permeability and porosity were measured after cleaning. Then the samples were evacuated and saturated with synthetic formation brine. After loading the sample and the porous plate into the core holder at an appropriate net stress, brine was flushed using a 500 psi back pressure to ensure a complete saturation. Resistivity was measured, followed by injection of

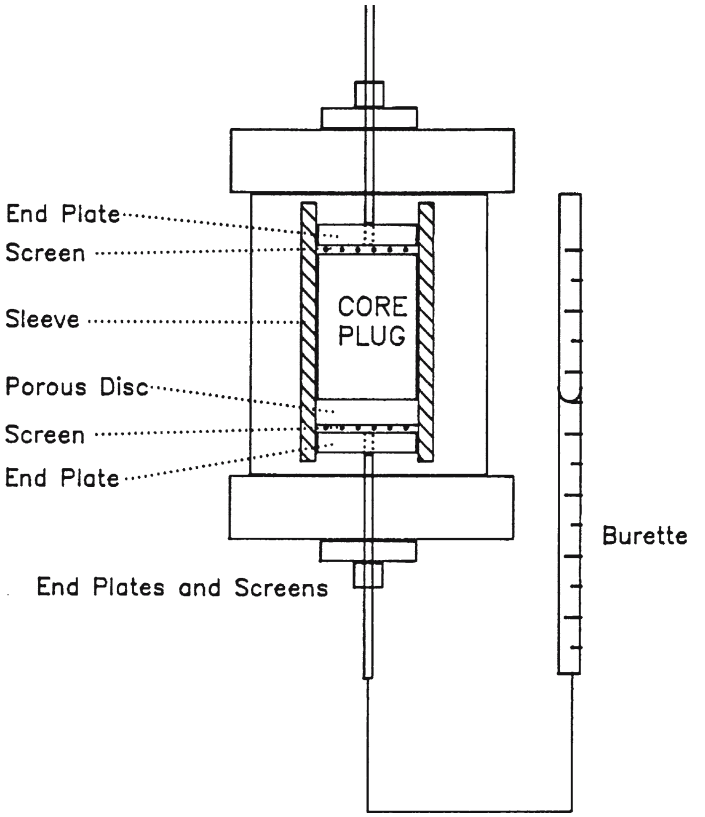

Figure 1. Schematic of experimental apparatus for measuring capillary pressure.

several pore volumes of brine. The resistivity at a water saturation of 100% was measured again the following day until stabilized (less than 1% change per day). Formation resistivity factor (FRF) at stress was determined at this point.

The sample was desaturated beginning at a low pressure by injecting humidified air at a regulated capillary pressure. The volume and weight of displaced brine were monitored and used to calculate the brine saturation. Resistivity, capillary pressure, and brine saturation were measured daily at each pressure point until saturation was stabilized (less than 1% change per day). This was repeated until no water was produced. At the end of the test, each sample was removed and its weight out was measured. It was Dean-Stark extracted for water, methanol soxhlet extracted for salts, and dried to a constant weight in a vacuum oven at 100°C. The final dry weight was measured. Dean-Stark water extracted was used to confirm the final water saturation.

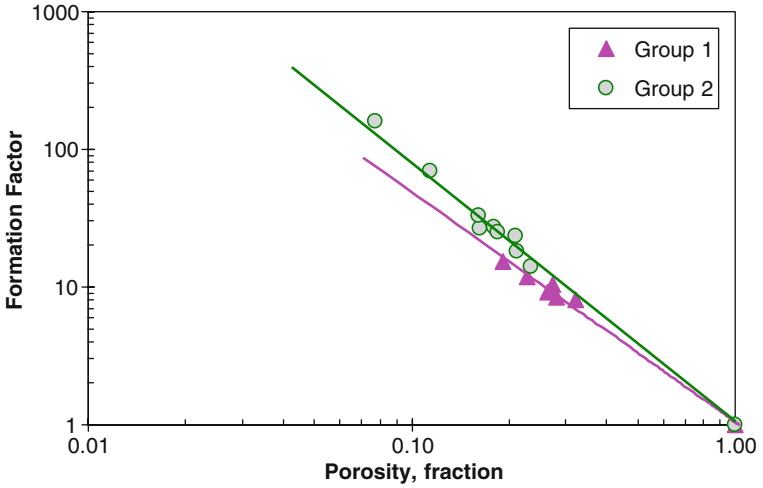

Figure 2. Relationship between formation factor and porosity for all of the core samples from two formations.

4. Results

The experimental data of capillary pressure and resistivity index in core samples from two formations in one oil reservoir were used to test the model (Equation 6) proposed in this study. The relative experimental error for measuring capillary pressure and resistivity was about 1.0%. The results are presented and discussed in this section.

Figure 2 shows the relationship between formation factor and porosity for all the samples from two formations. The results follow the first Archie's equation (Equation 9). The values of cement exponent were calculated using Equation 9: m is equal to 1.71 for the core samples in Group 1 (formation 1) and is equal to 2.19 for core samples in Group 2 (formation 2).

The data of resistivity index vs. water saturation for the core samples in Group 1 (high permeability) are shown in Figure 3. The data points follow the fractal model (Equation 2) and the Archie's saturation equation (Equation 8). The values of saturation exponent were calculated for each core sample using Equation 8 and the results are shown in Table I. The value of n ranges from 1.82 to 2.11 and the average value is about 1.94. The average value was calculated by conducting regression analysis for all of the data points.

For the core samples from the low permeability formation (Group 2), the experimental data of resistivity index are shown in Figure 4. One can see that the relationship between resistivity index and water saturation also follows the fractal model (Equation 2) and the Archie's saturation equation

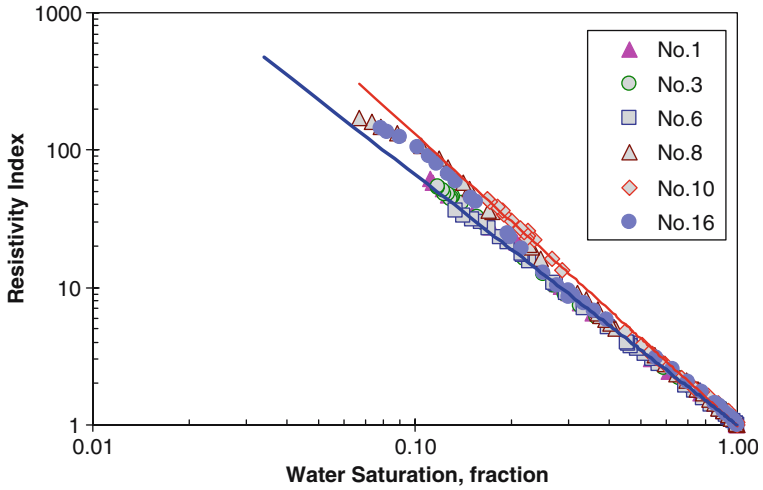

Figure 3. Relationship between resistivity index and water saturation for the core samples in Group 1.

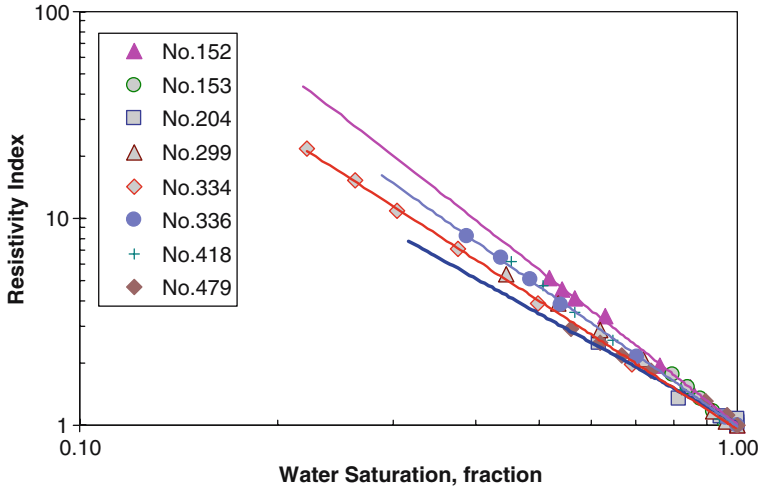

Figure 4. Relationship between resistivity index and water saturation for the core samples in Group 2.

(Equation 8). The values of saturation exponent calculated using Equation 8 are also listed in Table I. The value of n ranges from 1.82 to 2.49 and the average value is about 2.13.

It is important to demonstrate experimentally that the relationship between resistivity and water saturation follows the fractal model (Equation 2) and the Archie's saturation equation (Equation 8). This is because the relationship between capillary pressure and resistivity index (Equation 7) is

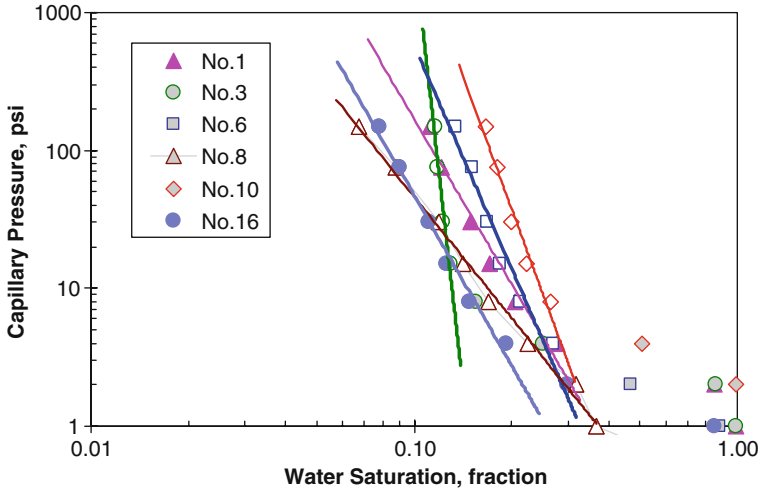

Figure 5. Capillary pressure curves of the core samples in Group 1 (high permeability).

derived based on the fractal model (Equation 2) and the Archie's saturation equation (Equation 8).

It is necessary to have the experimental data of capillary pressure to verify the model represented by Equation 6. The capillary pressure data of the core samples in Group 1 are shown in Figure 5. According to Equation 3, the relationship between capillary pressure and water saturation is linear on a log-log plot in the range of small water saturation. Figure 5 shows such a feature, which provides the evidence to support the model (Equation 3) proposed by Toledo *et al.* (1994). One can see from Figure 5 that the range of water saturation in which the linear relationship exists is different in different core samples. Note that the range of water saturation in which the linear relationship exists is very narrow for the No. 3 core sample (see Figure 5).

It is expected theoretically that the fractal dimension calculated using Equation 3 is in the range from 2 to 3 according to the fractal geometry. The greater the fractal dimension is, the greater the heterogeneity of the rock is. The values of fractal dimension were inferred from the capillary pressure data shown in Figure 5 by using Equation 3 and the results are listed in Table I. For the high permeability group core samples, the fractal dimension ranged from 2.599 to 2.952. The range of the calculated fractal dimension is consistent with the fractal theory. Core No. 3 had the greatest fractal dimension, which implies it was the most heterogeneous in this group.

The capillary pressure data of the core samples in Group 2 (low permeability) are shown in Figure 6. This figure also shows that the relationship between capillary pressure and water saturation is linear on a log-log plot.

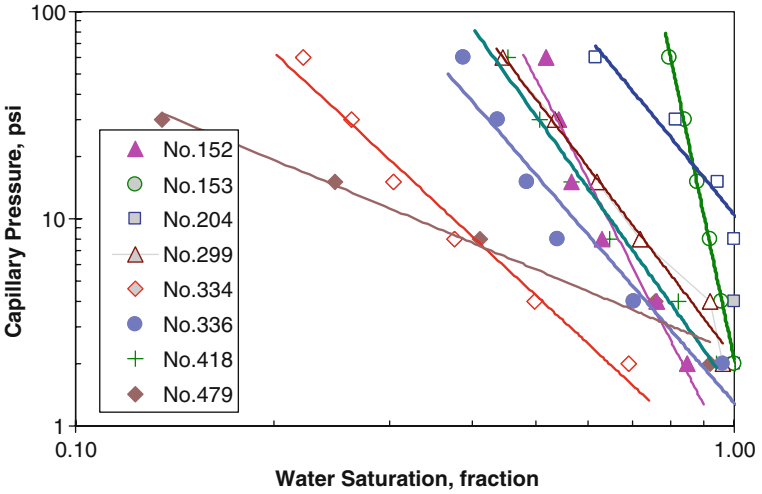

Figure 6. Capillary pressure curves of the core samples in Group 2 (low permeability).

The values of fractal dimension were also inferred from the capillary pressure data shown in Figure 6 by using Equation 3 and the results are listed in Table I. For the low permeability group core samples, the fractal dimension ranged from 2.287 to 2.824. The range of the calculated fractal dimension is also between 2.0 and 3.0, as expected from the fractal theory. Core No. 153 was the most heterogeneous in this group because it had the greatest fractal dimension.

One can see from Figures 5 and 6 that the range of water saturation in which the power law relationship exists is different in the two groups. For the core samples in Group 1 with a high permeability, the straight line crosses over only a narrow part with small water saturations. For the core samples in Group 2 with a low permeability, the straight line crosses over a much wider range of water saturation. For example, the range of water saturation in which the power law relationship exists is from 20% to about 70% for core sample No. 334. Within the same group, there is no evidence to show that the range of water saturation in which the power law relationship exists depends on permeability.

The experimental results shown in Figures 5 and 6 as well as the values of the calculated fractal dimension listed in Table I support the fractal scaling theory represented by Equation 3 in a specific range of water saturations.

The results listed in Table I do not show that there is any relationship between fractal dimension and permeability. This may be reasonable because permeability is not a parameter representing the heterogeneity of rock.

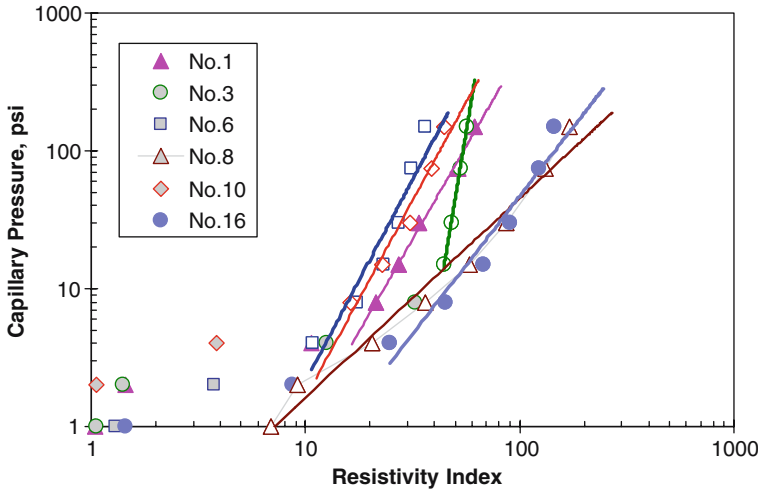

Figure 7. Relationship between capillary pressure and resistivity index in the core samples (Group 1, high permeability).

The relationships between capillary pressure and resistivity index of Groups 1 and 2 are shown in Figures 7 and 8 respectively. In Figure 7, a straight line can be fitted to the log-log plot in the range with great values of capillary pressure and resistivity index (corresponding to small water saturations). The values of fitting coefficient, R^2, are listed in Table I (Group 1). The fit was done in Figure 7 only for the values with high resistivity index. One can see from the values of fitting coefficient that the fitting is satisfactory in the range of great resistivity or low water saturation. For convenience, the critical water saturation (S_{wc}) is defined as the maximum water saturation in the range of water saturation in which the power law relationship exists. The critical water saturation was different in different rocks. Core sample No. 8 had the maximum critical water saturation of about 40% and core sample No. 3 had the minimum critical water saturation of about 15%.

Interestingly the number of the data points which are not on the straight line is much less in the core samples with a low permeability (see Figure 8) than in those with a high permeability. The range of water saturation in which the power law relationship exists is much wider in the core samples with a low permeability than that in the core samples with a high permeability (see Figures 7 and 8). This demonstrates that the model (Equation 6) derived from fractal modeling of a porous medium work better in core samples with a low permeability. Most of the core samples in Group 2 had a critical water saturation greater than 90%.

The values of regression coefficient (R^2), i.e., the goodness of fitting, of the model to the data shown in Figure 8 were also calculated and are listed

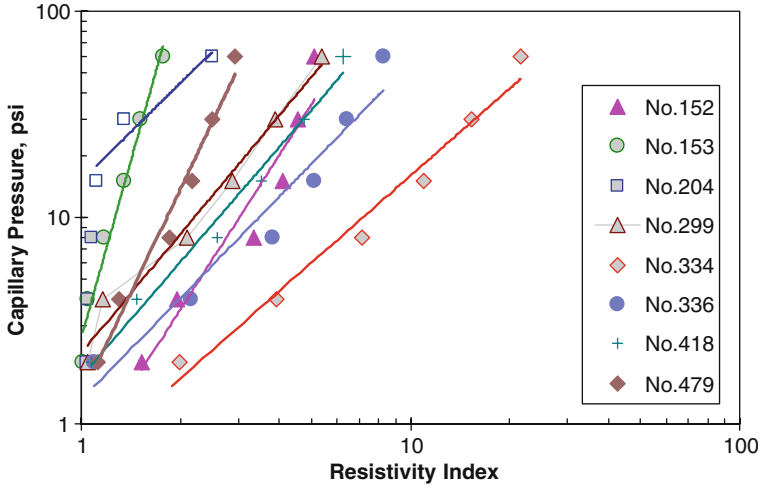

Figure 8. Relationship between capillary pressure and resistivity index in the core samples (Group 2, low permeability).

in Table 1. One can see that the goodness of fitting in Figure 8 is satisfactory too.

As stated previously, Szabo (1974) proposed a linear model (Equation 1) to correlate capillary pressure and resistivity by assuming the exponent of capillary pressure curve is equal to that of the resistivity index curve. This model was tested using the experimental data shown in Figures 7 and 8. The results did not show a linear relationship between capillary pressure and relative permeability (Equation 1) in the cases studied.

The values of β were calculated using Equation 6 with the data shown in Figures 7 and 8. The results are listed in Table 1. For most of the core samples, the value of β is in the range from 1 to 3. The effect of permeability on β for the core samples in both Group 1 and 2 is shown in Figures 9 and 10 respectively.

In the cases studied, for both Group 1 and 2, the value of β decreases with the increase in permeability. Note that core No. 3 is excluded in Figure 9 because the value of β is far off from the main trend. The values of the fitting coefficient for Group 1 and 2 are 0.82 and 0.71 respectively when a linear regression for the relationship between permeability and β was conducted in a log-log plot, as shown in Figures 9 and 10.

5. Discussion

As demonstrated in Figure 7, the power law model proposed in this study to correlate capillary pressure and resistivity works properly for high values of capillary pressure and resistivity (corresponding to low values of water

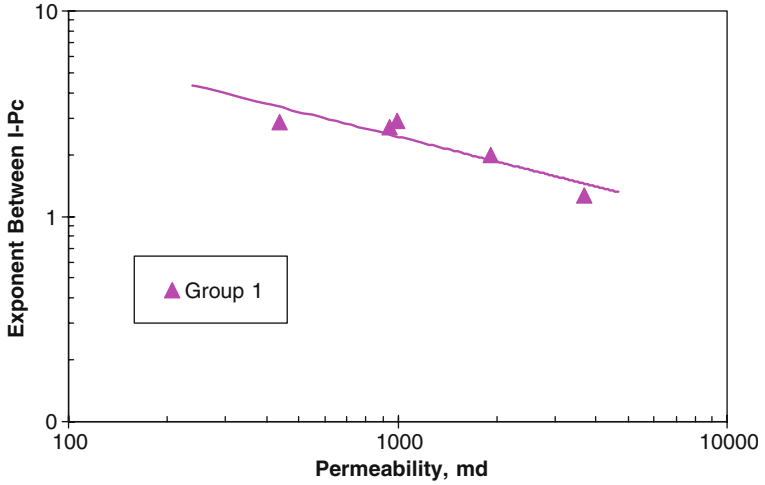

Figure 9. Effect of permeability on β for the core samples in Group 1 (low permeability).

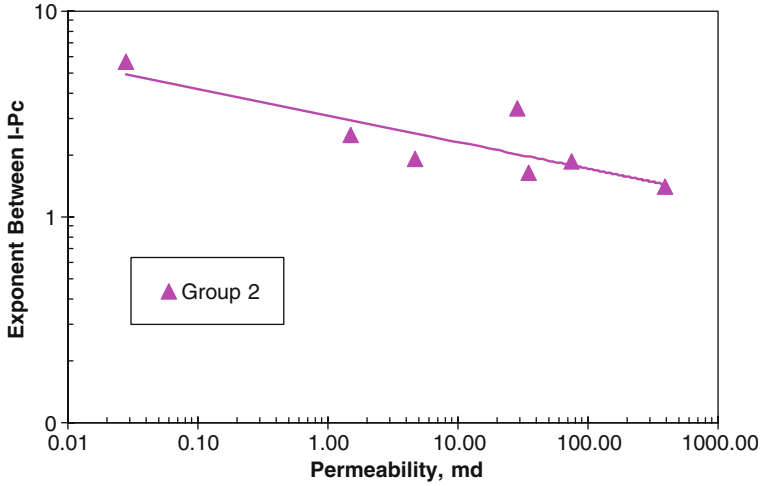

Figure 10. Effect of permeability on β for the core samples in Group 2 (high permeability).

saturations) in core samples with a high permeability. At high water saturations, the experimental data deviate the power law model. The possible reason may be that the distribution of water saturation may not be a fractal at high water saturations. In this case, water (wetting phase) remains in both small and big pores. It has been demonstrated that the part of the rock with big pores may not be a fractal (Katz and Thompson, 1985; Li, 2004). This was also pointed out by Toledo *et al.* (1994). Note that Equations 2 and 3 are only suitable for a specific range of water saturation with

low values. In the case of low permeability core samples, the number of data points that deviate the power law model is significantly less. This may be due to the unique fractal property of low permeability core samples. In low permeability rock, most of the pores are small and the pore system may be a fractal. When water (wetting phase) saturation is below a specific value (for example, the percolation threshold), water exists as thin films and follows the surface shape of pores in the rock, which is a fractal and the power law applies. However this may need to study in more detail.

Note that the linear model (Equation 1) proposed by Szabo (1974) can fit some of the experimental data for the high values of capillary pressure, especially in low permeability core samples. However the data points that fit the model are very few.

It is not uncommon to find systems with similar fractal dimension but with very different behavior. This difference may be characterized by lacunarity values (Mandelbrot, 1983; Plotnick *et al.*, 1996). However the model represented the relationship between capillary pressure and resistivity may become very complicated and may be difficult to use if the scale-dependent lacunarity values are used. On the other hand, the experimental results in this paper demonstrated that the model works satisfactorily with fractal dimension in a specific range of water saturation. This is why lacunarity values were not used in this study. It may be a good idea to study more on lacunarity in the future research.

6. Conclusions

The following conclusions may be drawn from the present study:

1. A model was developed theoretically to correlate capillary pressure and resistivity index. This model predicts a power law relationship between capillary pressure and resistivity index in a specific range of low water saturation.
2. The model derived in this study was tested against experimental data in 14 core samples from an oil reservoir. The permeability ranged from 0.028 to over 3000 md. The results demonstrated that the model work satisfactorily.
3. The model works better in core samples with low permeabilities than those with high permeabilities. The range of water saturation in which the power law relationship exists is much wider in the core samples with a low permeability than that in the core samples with a high permeability.
4. The value of β decreases with the increase in permeability. The relationship between permeability and β can be modeled approximately using a linear function in a log-log plot in the cases studied.

5. The experimental results support the fractal scaling theory represented by Equations 2 and 3 in a specific range of low water saturation. The values of fractal dimension inferred using Equation 3 ranged between 2 and 3.

Acknowledgements

This research was conducted with financial support from the US Department of Energy under grant DE-FG07–02ID14418, the contribution of which is gratefully acknowledged. The authors thank CoreLab for the permission to publish these results.

References

Archie, G.E.: 1942, The Electrical Resistivity Log as an Aid in Determining Some Reservoir Characteristics, *AIME* Petroleum Tech. 1–8.

Brooks, R. H. and Corey, A. T.: 1966, Properties of Porous Media Affecting Fluid Flow, *J. Irrig. Drain. Div.* **6,** 61.

Katz, A.J. and Thompson, A.H.: 1985, Fractal Sandstone Pores: Implications for Conductivity and Pore Formation, *Phys. Rev. Lett.*, **54**, 1325–1328.

Li, K.: 2004, *Characterization of Rock Heterogeneity Using Fractal Geometry*, SPE 86975, Proceedings of the 2004 SPE Western Region Meeting, March 16–18 Bakersfield, CA, USA.

Li, K.: 2005, *A Semianalytical Method to Calculate Relative Permeability from Resistivity Well Logs*, SPE 95575, the 2005 SPE Annual Technical Conference and Exhibition, October 9–12. Dallas, TX, USA.

Longeron, D.G., Argaud, M.J., and Bouvier, L.: 1989, *Resistivity Index and Capillary Pressure Measurements under Reservoir Conditions using Crude Oil*, SPE 19589, presented at the 1989 SPE Annual Technical Conference and Exhibition, October 8–11, San Antonio, TX, USA.

Mandelbrot, B.: 1983 *The Fractal Geometry of Nature*, Freeman, New York.

Plotnick, R.E., Gardner, R. H., Hargrove, W. W., Prestegaard, K., and Perlmutter, M.: 1996, Lacunarity analysis: A general technique for the analysis of spatial patterns, *Phys. Rev. E*, 53(5), 5461–5468.

Szabo, M.T.: 1974, New Methods for Measuring Imbibition Capillary Pressure and Electrical Resistivity Curves by Centrifuge, *SPEJ* (June) 243–252.

Toledo, G. T., Novy, R. A., Davis, H. T. and Scriven, L. E.: 1994, Capillary Pressure, Water Relative Permeability, Electrical Conductivity and Capillary Dispersion Coefficient of Fractal Porous Media at Low Wetting Phase Saturation, SPE Advanced Technology Series (SPE23675), **2**(1), 136–141.

Van Genuchten, M. T.: 1980, A Closed Form Equation for Predicting the Hydraulic Conductivity of Unsaturated Soils, *Soil Sci. Soc. Am. J.* **44,** 892-898.